

Supporting Information for:

In-situ (Bio)Remediation Treatment Options for U and Sr Contaminated Land: A Comparison of Radionuclide Retention and Remobilisation

Gianni F. Vettese^{a†}, Katherine Morris^a, Matthew White-Pettigrew^a, Luke T. Townsend^{a‡}, Samuel Shaw^a Christopher Boothman^a and Jonathan R. Lloyd^{*a}.

¹*Williamson Research Centre for Molecular Environmental Science and Research Centre for Radwaste Disposal, Department of Earth and Environmental Science, The University of Manchester, Manchester, England*

[†]*Present address: Radiochemistry Unit, Department of Chemistry, The University of Helsinki, Helsinki, Finland*

[‡]*Present address: Immobilisation Science Laboratory, Department of Materials Science and Engineering, University of Sheffield, Sheffield S1 3JD, UK*

The SI contains 12 pages, 12 figures and 2 tables.

SI 1: Sediment and Synthetic Groundwater Composition

The sediments used in this study were taken from the same location as ^{1,2}. The sediment mineralogy was composed mostly of silicate minerals including quartz (SiO_2), sheet silicates (muscovite, $[\text{KAl}_2(\text{Si}_3\text{Al})\text{O}_{10}(\text{OH},\text{F})_2]$) and clinocllore, $[(\text{Mg},\text{Fe}^{2+})_5\text{Al}_2\text{Si}_3\text{O}_{10}(\text{OH})_8]$), feldspars (Albite, $[\text{NaAlSi}_3\text{O}_8]$) and microcline, $[\text{KAlSi}_3\text{O}_8]$) and iron oxides (hematite, $[\text{Fe}^{3+}_2\text{O}_3]$). X-ray fluorescence analysis showed that the sediment contained (wt%): Si (63.1), Al (15.7), Fe (6.5), K (4.9), Mg (2.2), Na (1.3), Ca (0.7), Ti (0.7), Mn (0.2), P (0.1) and other trace metals at concentrations below 0.1 wt%. The proportion of organic C lost as CO_2 was determined by loss on ignition, as 4.1 wt%.

SI 2: pH and Eh

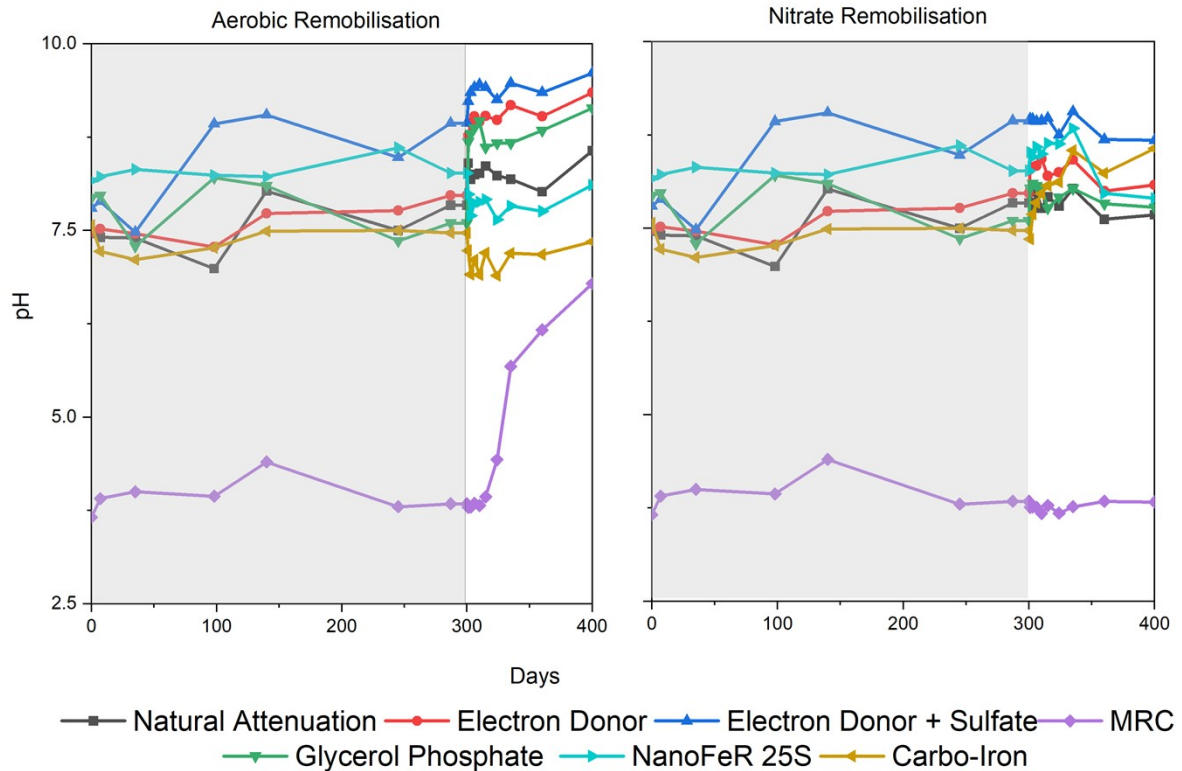


Figure SI1: Changes in pH across all experiments. Incubation phases are highlighted in grey and remobilisation phases are left blank.

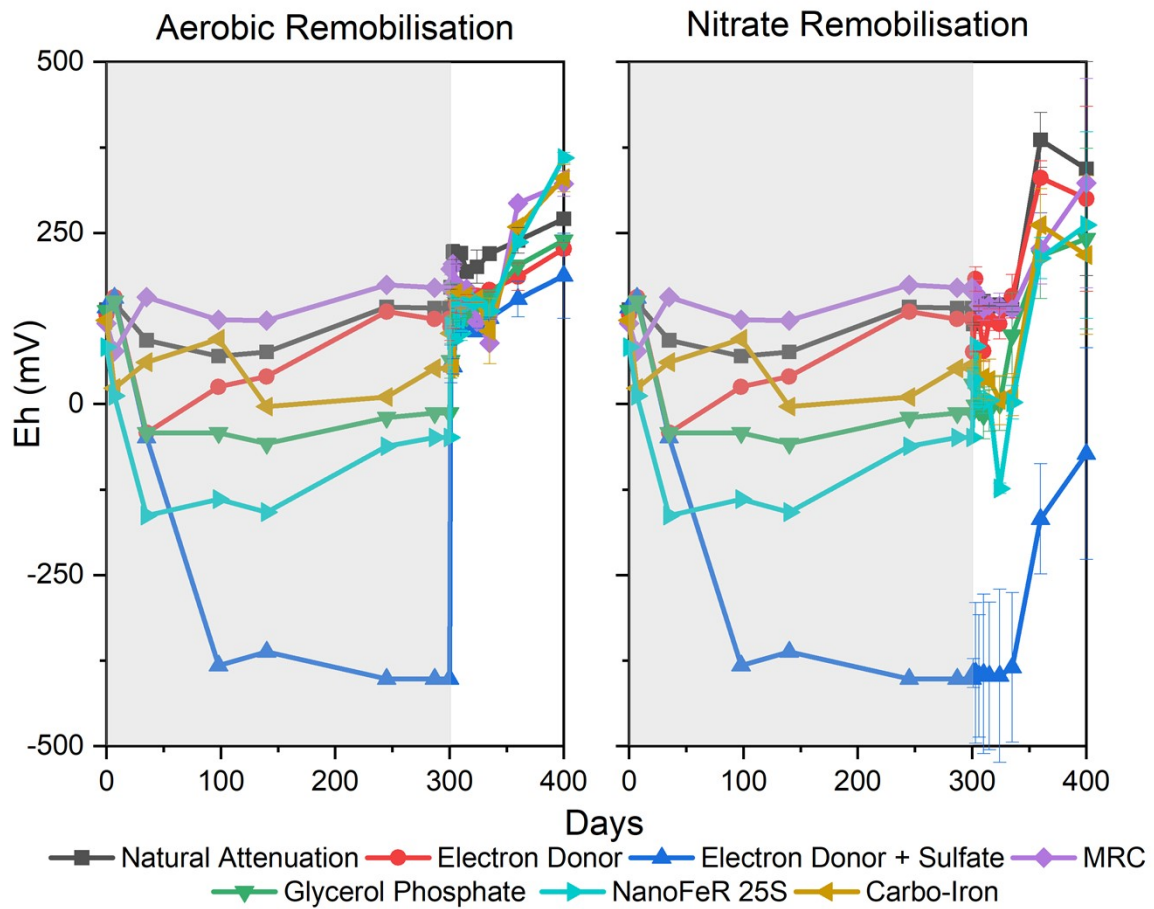


Figure SI 2: Eh values across all experiments. Incubation phases are highlighted in grey and remobilisation phases are left blank. Error bars represent 1 standard deviation based on triplicate measurements.

SI 3: Ion Chromatography

Although nitrate, nitrite, phosphate, glycerol phosphate, sulfate and volatile fatty acids were all measured using ion chromatography (IC), here we present selected IC results from the batch incubation and the remobilisation studies. Monitoring aqueous phosphate and nitrate using a Dionex ICS 5000 with an AS18 2 mm ion exchange column at 0.25 mL/min and monitoring sulfate, nitrite, glycerol phosphate and volatile fatty acids using a Dionex ICS 5000 with an AS11HC 0.4 mm high-capacity ion exchange column at 0.015 mL/min.

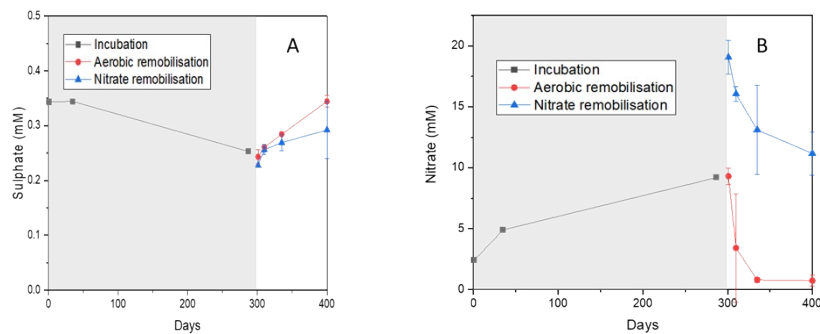


Figure SI 3: (A) Sulfate; and (B) nitrate concentrations in the natural attenuation experiments. With data for the incubation phase (black lines) and remobilisation data for each species after aeration (red lines) or when amended with nitrate (blue lines). Measurements were performed in triplicate with error bars representing 1 standard deviation (σ). Incubation phases are highlighted in grey and remobilisation phases are left blank.

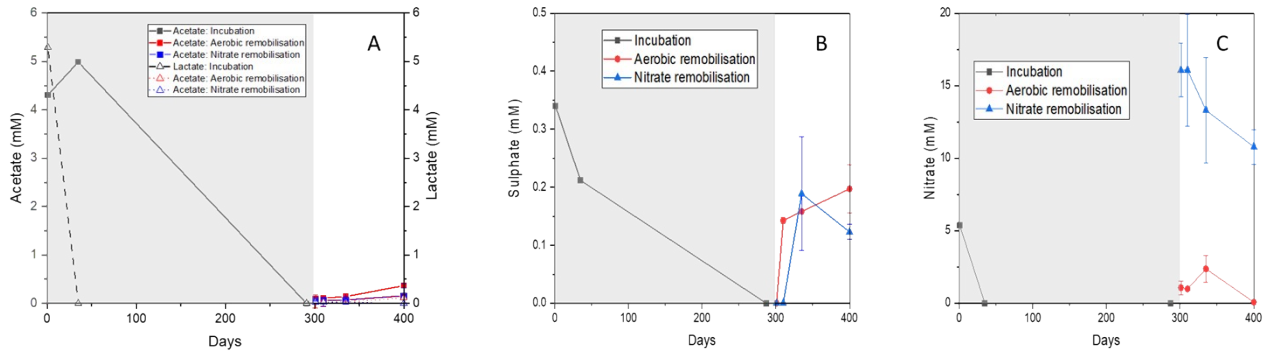


Figure SI 4: (A) Acetate (left axis) and Lactate (right axis); (B) sulphate; and (C) nitrate concentrations in the electron donor experiments. With data for the incubation phase (black lines) and remobilisation data for each species after aeration (red lines) or when amended with nitrate (blue lines). Measurements were performed in triplicate with error bars representing 1 standard deviation (σ). Incubation phases are highlighted in grey and remobilisation phases are left blank.

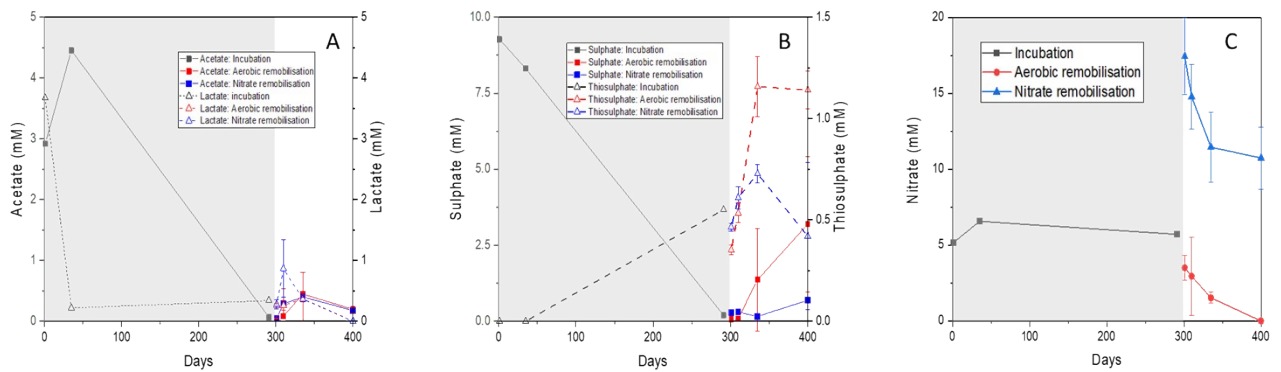


Figure SI 5: (A) Acetate (left axis) and Lactate (right axis); (B) sulphate; and (C) nitrate concentrations in the electron donor plus sulfate experiments. With data for the incubation phase (black lines) and remobilisation data for each species after aeration (red lines) or when amended with nitrate (blue lines). Measurements were performed in triplicate with error bars representing 1 standard deviation (σ). Incubation phases are highlighted in grey and remobilisation phases are left blank.

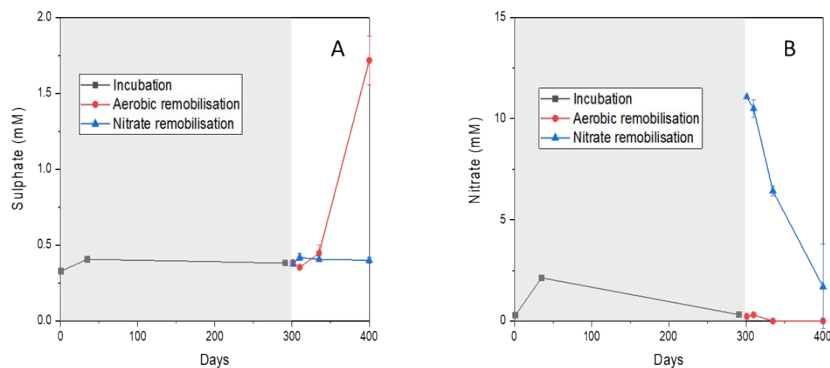


Figure SI 6: (A) Sulfate; and (B) nitrate concentrations in the MRC experiments. With data for the incubation phase (black lines) and remobilisation data for each species after aeration (red lines) or when amended with nitrate (blue lines). Measurements were performed in triplicate with error bars representing 1 standard deviation (σ). Incubation phases are highlighted in grey and remobilisation phases are left blank.

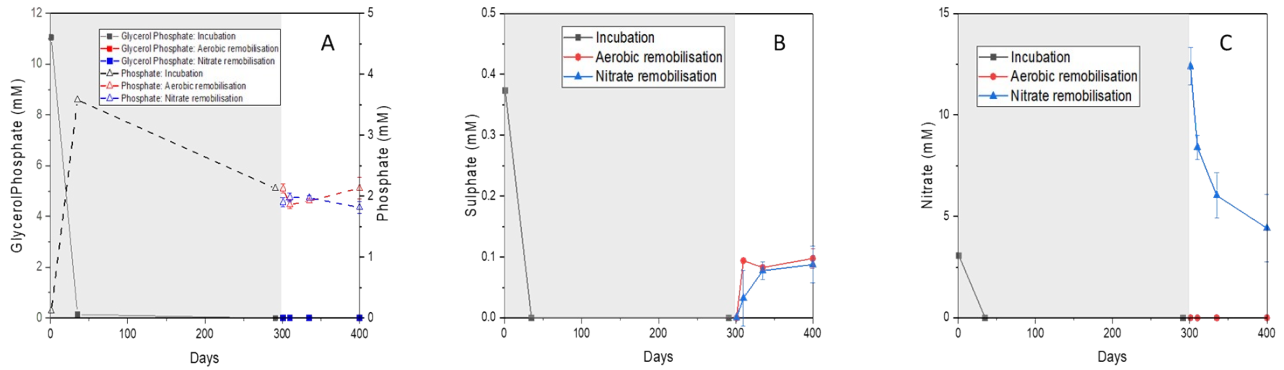


Figure SI 7: (A) Glycerol phosphate (left axis) and phosphate (right axis); (B) sulphate; and (C) nitrate concentrations in the glycerol phosphate experiments. With data for the incubation phase (black lines) and remobilisation data for each species after aeration (red lines) or when amended with nitrate (blue lines). Measurements were performed in triplicate with error bars representing 1 standard deviation (σ). Incubation phases are highlighted in grey and remobilisation phases are left blank.

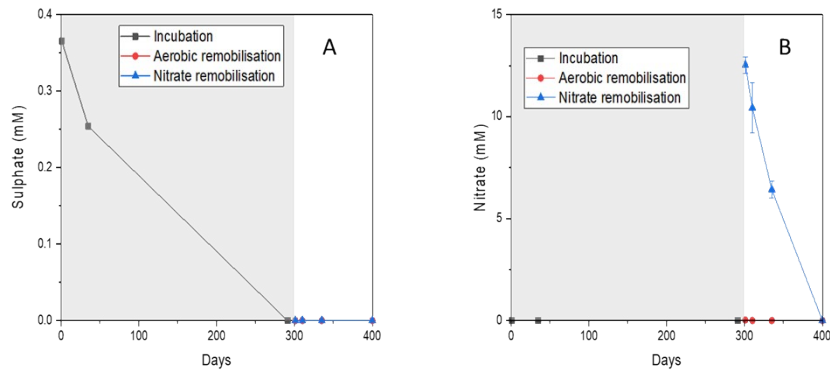


Figure SI 8: (A) Sulfate; and (B) nitrate concentrations in the NANOFR 25S experiments. With data for the incubation phase (black lines) and remobilisation data for each species after aeration (red lines) or when amended with nitrate (blue lines). Measurements were performed in triplicate with error bars representing 1 standard deviation (σ). Incubation phases are highlighted in grey and remobilisation phases are left blank.

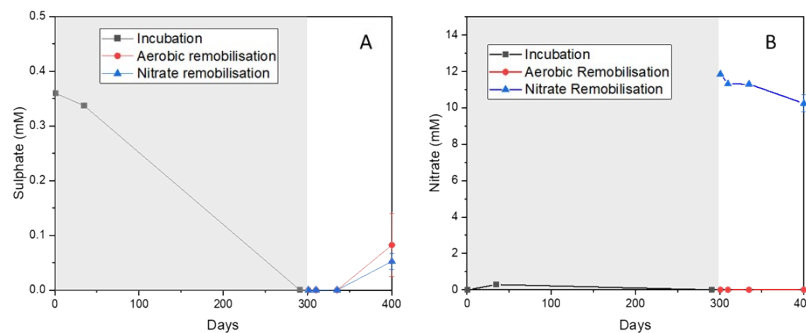


Figure SI 9: (A) Sulfate; and (B) nitrate concentrations in the Carbo-Iron experiments. With data for the incubation phase (black lines) and remobilisation data for each species after aeration (red lines) or when amended with nitrate (blue lines). Measurements were performed in triplicate with error bars representing 1 standard deviation (σ). Incubation phases are highlighted in grey and remobilisation phases are left blank.

SI 4: Additional X-ray Absorption Spectroscopy Data and Analysis

During data acquisition beam damage was assessed by measuring several quick X-ray Absorption Near-Edge Structure (XANES) spectra, exposing the sample and analysing the spectral features (peak height, position and intensities) in order to assess any evidence for oxidation state drift. Throughout, we did not see any evidence for beam damage effects.

XANES

Before EXAFS fitting was carried out, linear combination fitting of the U L₃-edge XANES was used to inform the U(VI):U(IV) ratios. Linear combination fitting of all samples was performed using U(VI), as uranyl(VI) triscarbonate⁴, and U(IV), as uraninite⁵, except for the glycerol phosphate amended system which used U(VI) and U(IV) phosphate standards^{6,7}. Whilst U(V) has been identified under environmentally relevant conditions⁸⁻¹⁷, U L₃-edge analyses are not sufficient to unambiguously identify U(V)¹⁷⁻¹⁹, thus for this data set U has been assumed to be either U(VI), or U(IV). As Sr is non redox active LCF was not carried out and all Sr was assumed to be Sr(II).

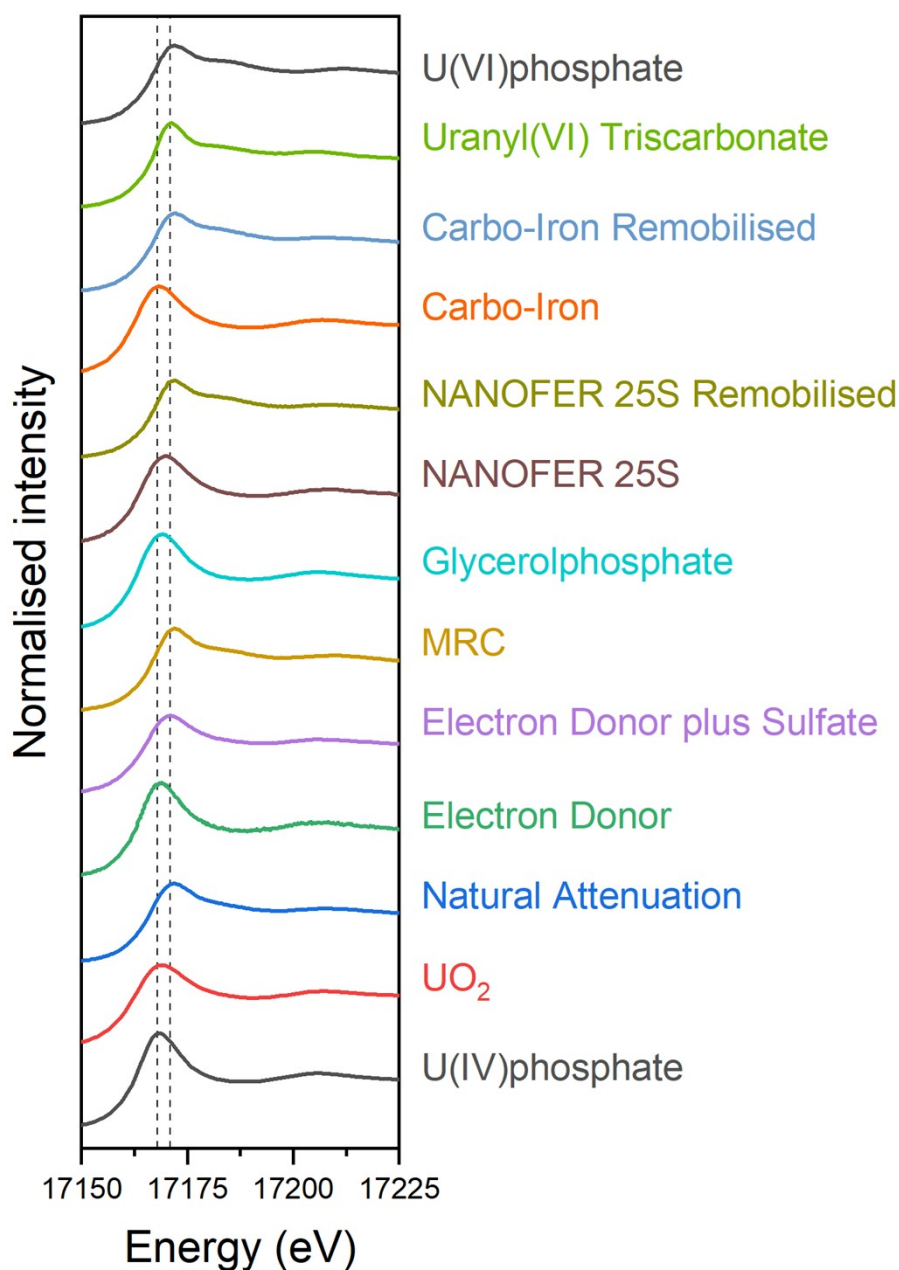
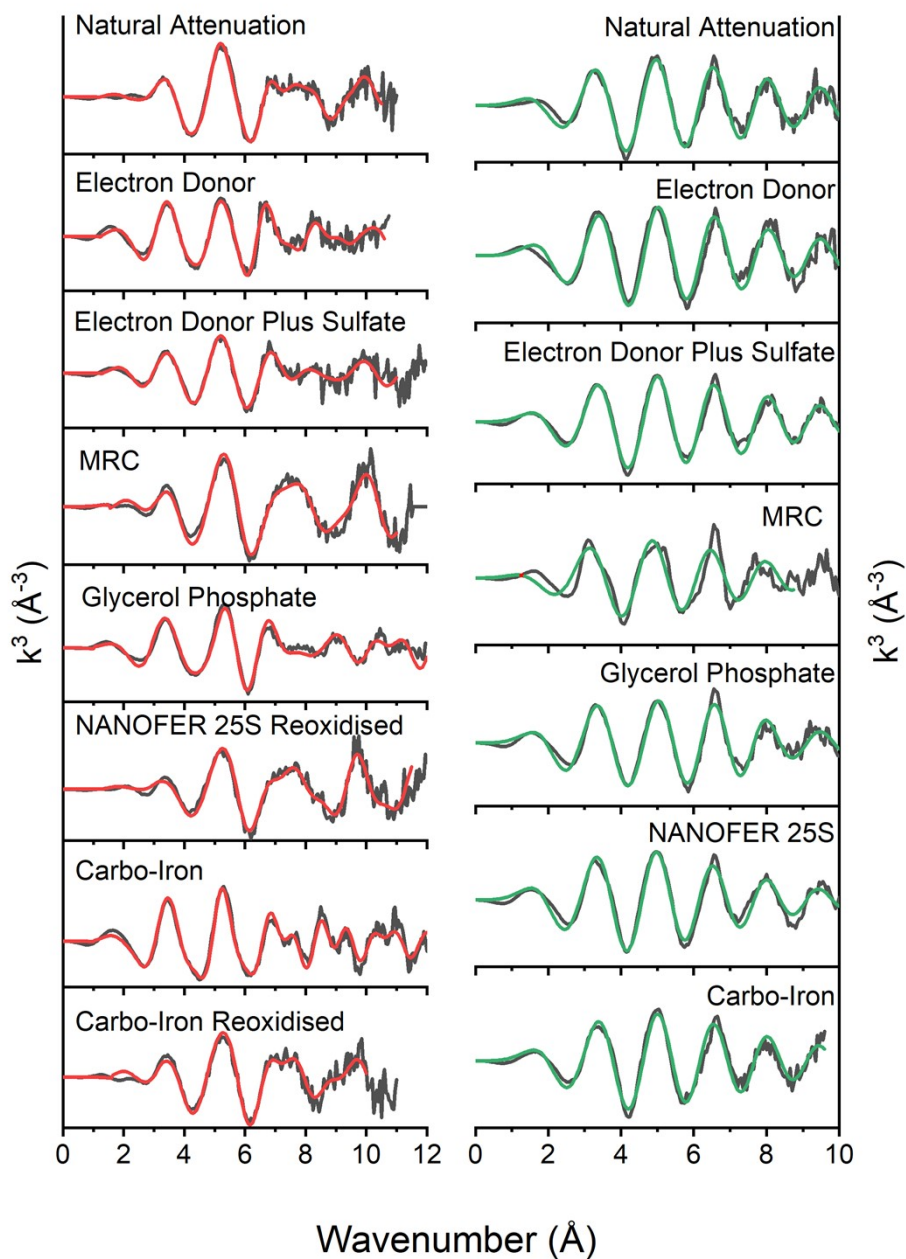


Figure SI 10: U L₃-edge XANES spectra collected at 77 K. Standards: Uranyl(VI) triscarbonate from ⁴, U(VI) phosphate from ⁶ U(IV) phosphate from ⁷, synthetic U(IV)O₂ standard from ⁵. Dashed lines at 17168 eV and 17171 eV indicate U(IV) and U(VI) white lines respectively.

EXAFS Fitting

The U L₃-edge EXAFS spectra were quantitatively fitted using the phase shift and backscattering functions obtained using the published reference structures of liebigite, Ca₂[UO₂(CO₃)₃] · ~11H₂O ²⁰; ningyoite [CaU(PO₄)₂·2H₂O] ²¹; [U(SO₄)₂·4H₂O] ²²; Magnetite (Fe₃O₄) ²³; and uraninite, UO₂ ²⁴ were used. The Sr K-edge EXAFS spectra were quantitatively fitted using the phase shift and backscattering functions obtained using published reference structures of strontianite, SrCO₃ ²⁵ and strontium hydroxide phosphate, Sr₅(PO₄)₃OH, which is isostructural with hydroxyapatite Ca₅(PO₄)₃OH ²⁶. The R-factor value was used in this study to evaluate the quality of fits and additional shells were only included in the fit if they made a statistically significant improvement to the model fit

as determined by the F-test²⁷. 9-coordinate outer-sphere sorbed Sr to oxygen ligands was used a reasonable base for Sr EXAFS and



similarly, further shells were only added if they contributed statistically to the fits²⁷.

Figure SI 11: EXAFS in k^3 (black) and fits U L_3 -edge (left, red) and for Sr K-edge (right, green).

Table SI 1: Fitting Parameters obtained from Uranium L_3 -Edge and Sr-K-edge EXAFS Spectroscopy.

U EXAFS Fits							
	Scattering path	N	R (Å)	σ^2 (Å ²)	E_0 (eV)	R-factor	Confidence of adding shell (%) ^a
Natural Attenuation Control	U=O _{axial}	1.4	1.78(2)	0.003(2)	4.30	0.009	
	U(IV)-O	2.6	2.25(1)	0.004(1)			

	U(VI)-O _{equatorial}	4.2	2.41(4)	0.003(1)			
Electron Donor	U-O	8	2.40(1)	0.013(1)	6.28	0.011	
	U-P _{bidentate}	1	3.13(2)	0.003(2)			98.9
	U-P _{monodentate}	2	3.68(3)	0.005(3)			99.3
	U-U	3	3.99(4)	0.012(4)			97.1
Electron Donor Plus Sulfate	U=O _{ax}	0.8	1.81(1)	0.005(2)	6.93	0.017	
	U(IV)-O	4.8	2.37(4)	0.016(8)			
	U(VI)-O _{eq}	2.4	2.43(4)	0.006(2)			
	U-P	1	3.15(3)	0.008(4)			98.8
MRC	U=O _{axial}	2	1.79(1)	0.002(1)	6.96	0.018	
	U-O _{equatorial}	6	2.39(3)	0.013(4)			
	U-S	1	3.16(4)	0.004(2)			96.5
Glycerol phosphate	U-O	4	2.28(2)	0.003(0)	4.07	0.020	
	U-O	4	2.44(2)	0.003(0)			
	U-P _{bidentate}	2	3.13(2)	0.004(2)			
	U-P _{monodentate}	4	3.67(3)	0.006(3)			
NANOFER 25S Aerobically Remobilised	U=O _{axial}	2	1.80(2)	0.003(1)	5.72	0.020	
	U-O _{equatorial}	2	2.20(3)	0.003(2)*			
	U-O _{equatorial}	4	2.40(3)	0.003(2)*			
	U-C	1.6	2.92(5)	0.002(1)			
	U-Fe	1	3.46(4)	0.002(1)			95.7
Carbo-Iron	U-O	4	2.28(2)	0.007(2)	3.85	0.018	
	U-O	3	2.44(1)	0.007(1)			
	U-Fe	1	3.45(3)	0.016(1)			98.0 ^b
	U-U	5	3.85(2)	0.011(7)			
Carbo-Iron Aerobically Remobilised	U=O _{axial}	2	1.83(1)	0.006(1)	5.70	0.022	
	U(VI)-O _{equatorial}	3	2.27(1)	0.003(2)			
	U(VI)-O _{equatorial}	3	2.45(1)	0.001(1)			
	U-Fe	1	3.45(3)	0.009(3)			98.2
Sr EXAFS Fits							

	Scattering path	N	R (Å)	σ^2 (Å ²)	E ₀	R-factor	Confidence of adding shell (α) ^a
Natural Attenuation Control	Sr-O	9	2.60(1)	0.009(1)	-0.03	0.016	
Electron Donor	Sr-O	9	2.61(1)	0.009(1)	-0.37	0.009	
Electron Donor Plus Sulfate	Sr-O	9	2.60(1)	0.009(0)	-0.67	0.009	
Glycerol phosphate	Sr-O	9	2.61(1)	0.011(6)	-0.17	0.008	96.3
	Sr-P	1.3	3.30(3)	0.013(4)			
MRC	Sr-O	9	2.58(3)	0.012(2)	-6.97	0.021	
NANOFER 25S	Sr-O	9	2.60(1)	0.0010(1)	-0.03	0.015	
Carbo-Iron	Sr-O	9	2.61(2)	0.010(1)	+0.40	0.019	

N is the coordination number, **R** is the interatomic distance, σ^2 is the Debye-Waller factor, **E₀** refers to the change in absorption energy, and **R-factor** describes the goodness of fit. Uncertainty in interatomic distances is quoted in brackets for the last decimal place (Å), points without a value have error less than 0.005 Å. Uncertainty in Debye-Waller factors is quoted in brackets for the last decimal place, points without a value have error less than 0.0005. ^a F-test results; $\alpha > 0.95$ statistically improves the fit with 2 σ confidence. ^b F-test results, shell added first. ^c F-test results, shell added second. Values marked with an * were tied together. S_0^2 was fixed to 1 for all samples, except for the U fits amended with MRC where S_0^2 was fixed to 0.9.

SI 5: Microbial Community Characterisation

The microbial community was assessed using standard procedures^{28–32}. Here, DNA was extracted from 200 μ l of sediment slurry or microcosm sample using a DNeasy PowerLyzer PowerSoil Kit (Qiagen, Manchester, U.K). Sequencing of PCR amplicons of 16S rRNA was conducted with the Illumina MiSeq platform (Illumina, San Diego, CA, USA) targeting the V4 hyper variable region (forward primer, 515F, 5'-GTGYCAGCMGCCGCGTAA-3'; reverse primer, 806R, 5'-GGACTACHVGGGTWTCTAAT-3') for 2 \times 250-bp paired-end sequencing (Illumina)^{33,34}. PCR amplification was performed using Roche FastStart High Fidelity PCR System (Roche Diagnostics Ltd, Burgess Hill, UK) in 50 μ l reactions under the following conditions: initial denaturation at 95°C for 2 min, followed by 36 cycles of 95°C for 30 s, 55°C for 30 s, 72°C for 1 min, and a final extension step of 5 min at 72°C. The PCR products were purified and normalised to approximately 20ng each using the SequelPrep Normalization Kit (Fisher Scientific, Loughborough, UK). The PCR amplicons from all samples were pooled in equimolar ratios. The run was performed using a 4 pM sample library spiked with 4 pM PhiX to a final concentration of 10% following the method of Schloss and Kozich³⁵.

Raw sequences were divided into samples by barcodes (up to one mismatch was permitted) using a sequencing pipeline. Quality control and trimming was performed using Cutadapt³⁶, FastQC³⁷, and Sickle³⁸. MiSeq error correction was performed using SPADes³⁹. Forward and reverse reads were incorporated into full-length sequences with Pandaseq⁴⁰. Chimeras were removed using ChimeraSlayer⁴¹, and OTUs were generated with UPARSE⁴². OTUs were classified by Usearch⁴³ at the 97% similarity level, and singletons were removed. Rarefaction analysis was conducted using the original detected OTUs in Qiime⁴⁴. The taxonomic assignment was performed by the RDP naïve Bayesian classifier version 2.2⁴⁵. The OTU tables were rarefied to the sample containing the lowest number of sequences, all samples having less than 5,000 sequences were removed from analyses prior to the rarefaction step. The step size used was 2000 and 10 iterations were performed at each step.

Table SI 2: Details of molecular ecology sequencing results.

Sample	Day	Number of Reads (OTUs)	Sequences per Sample at 10200	OTUs that are	Counts of Archaea
--------	-----	------------------------	-------------------------------	---------------	-------------------

			Reads	Archaea (%)	(OTUs)
Control		102393	935.7	0.12	17
Natural	300	122670	1322.8	0.25	36
Attenuation	400 – Aerobic	342366	1182.8	0.21	17
Control	400 – Nitrate	117257	1286.9	0.21	22
Electron Donor	300	101360	1372.7	1.79	28
	400 – Aerobic	130270	1293.4	9.30	18
	400 – Nitrate	123907	1132.3	0.42	26
Electron Donor	300	110927	700.4	0.33	19
Plus Sulfate	400 – Aerobic	114302	1050.5	12.42	13
	400 – Nitrate	82678	454.7	0.41	19
MRC	300	86973	423.8	0.26	25
	400 – Aerobic	118171	693.2	0.23	21
	400 – Nitrate	129363	419.2	9.85	25
Glycerol	300	120316	555.2	8.32	6
Phosphate	400 – Aerobic	15578	214.9	1.51	4
	400 – Nitrate	108666	236.5	0.40	12
NANOFER 25S	300	132066	845	0.33	15
	400 – Aerobic	132504	680.6	0.20	5
	400 – Nitrate	146088	566.2	0.38	16
Carbo-Iron	300	84462	339.1	0.75	8
	400 – Aerobic	134433	592.7	0.47	11
	400 – Nitrate	119357	393.1	14.02	14

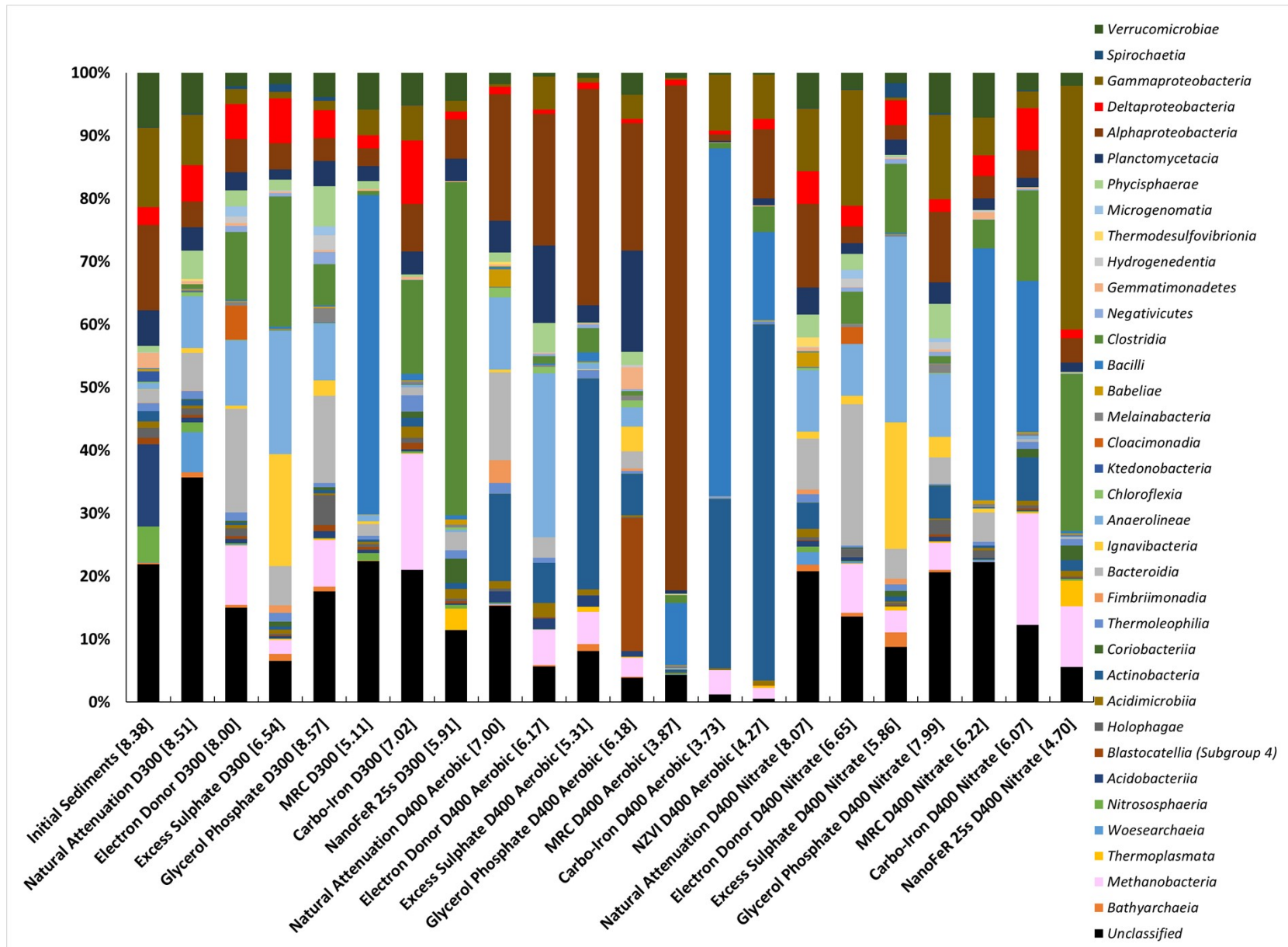


Figure SI 12: 16S rRNA gene sequencing results sorted by phylogenetic class. With Shannon indices in square brackets.